Targeting aberrant fatty acid synthesis and storage in endocrine resistant breast cancer cells

Ashley V. Ward[1], Duncan Riley[1], Jessica Finlay-Schultz[1], Heather M. Brechbuhl[2], Kaitlyn B. Hill[3], Rohan R. Varshney[3], Peter Kabos[2], Michael C. Rudolph[3#], and Carol A. Sartorius[1#*]

[1] University of Colorado, Anschutz Medical Campus; Department of Pathology; Aurora, CO, United States. (ashley.2.ward@cuanschutz.edu)

[2] University of Colorado, Anschutz Medical Campus; School of Medicine; Department of Medical Oncology; Aurora, CO, United States.

[3] University of Oklahoma Health Sciences Center, Harold Hamm Diabetes Center; Oklahoma City, OK, United States.

# these authors contributed equally

*Correspondence

Carol A Sartorius

Carol.Sartorius@cuanschutz.edu

Key words: Breast cancer; endocrine resistance, lipid metabolism; fatty acid; lipidomics; fatty acid synthase

Abstract

Background: Lipid metabolic reprogramming is an emerging characteristic of endocrine therapy (ET) resistance in estrogen receptor-positive (ER+) breast cancer. We explored changes in lipid metabolism in ER+ breast cancer cell lines following acquired resistance to common endocrine treatments and tested efficacy of an inhibitor in current clinical trials. ,

Methods: We derived ER+ breast cancer cell lines resistant to Tamoxifen (TamR), Fulvestrant (FulvR), and long-term estrogen withdrawal (EWD). Parental and ET resistant cells were subjected to global gene expression and unbiased lipidomic profiling. Lipid storage changes were assessed via neutral lipid staining with Oil Red O (ORO). The impact of the fatty acid synthase (FASN) inhibitor TVB-2640 on the growth and lipid storage of these cell lines was evaluated. Additionally, $^{13}C_2$-acetate tracing was used to examine FASN activity in parental and ET resistant cells in the absence or presence of TVB-2640.

Results: Compared to parental cells, lipid metabolism and processing pathways were notably enriched in ET resistant cells, which exhibited distinct lipidomes characterized by increased triglyceride and polyunsaturated FA (PUFA) species. ET-resistant cells displayed enhanced cytoplasmic lipid droplets. Increased FASN protein levels were observed in ET-resistant cells, and TVB-2640 effectively inhibited FASN activity. FASN inhibition reduced cell growth in some but not all cell lines and ET resistance types and did not correlate to lipid storage reduction. $^{13}C_2$-acetate tracing confirmed reduced palmitate synthesis and enhanced PUFA synthesis in ET-resistant cells, especially when combined with FulvR.

Conclusion: ET resistant breast cancer cells exhibit a shift towards enhanced triglyceride storage and complex lipids enriched with PUFA acyl chains. While targeting FASN alongside ET may not fully overcome ET resistance in our models, focusing on the unique lipid metabolic

47 dependencies, such as PUFA pathways, may present a promising alternative strategy for treating
48 ET resistant breast cancer.
49
50
51
52 **Background**
53
54 Overcoming resistance to endocrine therapies (ET) represents a pivotal challenge for
55 enhancing treatment outcomes in women with estrogen receptor-alpha (ER) positive breast
56 cancer, contributing to approximately half of all fatalities from the disease [1]. ET encompasses
57 three general classes of drugs: selective ER modulators (SERMS, e.g., Tamoxifen, (Tam)) that
58 disrupt binding of estrogens to ER, selective ER degraders (SERDs, e.g., Fulvestrant (Fulv)) that
59 cause immobilization and/or degradation of ER [2], and aromatase inhibitors that block
60 production of 17β-estradiol. Typically administered as adjuvant therapy over 5-10 years, ET
61 offers long-term disease stabilization or eradication for most patients. Unfortunately, acquired
62 ET resistance emerges in up to one third of women either during treatment or upon its
63 conclusion, often coinciding with distal metastasis [3]. At this time, several targeted therapies
64 may be integrated in combination with ET, including cyclin dependent kinases 4/6 inhibitors (i.e.
65 palbociclib), alpelisib for PIK3CA mutations, or the SERD elacestrant for tumors harboring ER
66 mutations [4, 5]. However, the development of acquired multidrug resistance is usually
67 inevitable. Consequently, an urgent need exists to identify new vulnerabilities in ET resistant
68 cells that can be effectively targeted in combination with endocrine drugs to mitigate the
69 recurrence risk or delay progression of recurrent disease.

70 ER+ breast cancers exhibit pronounced lipogenesis, utilizing de novo fatty acid (FA)
71 synthesis despite the presence of abundant FAs in their microenvironment [6]. FAs originating de
72 novo or from preformed sources facilitate synthesis of more complex lipids necessary for
73 membrane expansion, provide fuel for rapid tumor growth, and act as signaling molecules.
74 Central to this process is the upregulation of Sterol Regulatory Element-binding transcription
75 factor 1 (SREBP1) by estrogens, which in turn boosts the expression of two vital de novo FA
76 synthesis enzymes necessary in this pathway: acetyl-CoA carboxylase (ACC) and fatty-acid
77 synthase (FASN) [7]. ACC catalyzes the conversion of acetyl-CoA into malonyl-CoA, and both
78 precursors are needed for further catalysis by FASN to synthesize palmitate. Palmitate and
79 further elongated FAs are subsequently combined with preformed FA taken up from the
80 microenvironment by transporters, and together, they are subsequently incorporated into
81 triglycerides and frequently stored as cytoplasmic lipid droplets (LD) in breast cancer cells [8-
82 10]. This dual mode of FA synthesis and FA uptake underscores the complexity of targeting FA
83 dependence in breast cancers, especially given the adaptability in the metabolic incorporation of
84 these essential molecules that provide an advantage to cancer cells.
85 Recent studies have shown that lipid metabolic pathways undergo further alteration with
86 the development of ET resistance, with a significant body of research centering on Tam, the
87 longest approved breast cancer drug [11]. Hultsch et al. observed that Tam-resistant breast cancer
88 cells had a significant increase in triglycerides and cholesterol esters, stored in large LDs and
89 lysosomes, respectively [7, 8, 12, 13]. Moreover, ER+ invasive lobular carcinoma cells, resistant
90 to long term estrogen deprivation, exhibited heightened activation of lipid metabolism that could
91 be stratified into two distinct lipid pathways, SREPB1-activated FA synthesis or cholesterol
92 metabolism [14]. Notably, MCF7 cells subjected to long-term estrogen deprivation experience an

93 uptick in cholesterol biosynthesis [15]. HER2-overexpressing MCF7 variants had elevated FASN
94 expression alongside an increased dependency on lipid biosynthesis [7].
95 While multiple potential targets within lipid metabolism are promising, FASN inhibition
96 has historically received the most attention. FASN levels are consistently higher in breast cancer
97 compared to normal cells and breast tumor vs normal tissue [16]. While early-generation FASN
98 inhibitors demonstrated potential efficacy for tumor growth restriction in preclinical breast
99 cancer models, their clinical translation was limited due to substantial toxicity observed in both
100 animal models and human trials [17]. However, a more recently developed selective and
101 reversible FASN inhibitor (TVB-2640) has shown promising results, including dose-dependent
102 efficacy in advanced solid tumors like HER2-positive breast cancers and has advanced to Phase
103 II clinical trials [18]. Beyond FASN, other targets within lipid metabolism are currently being
104 explored, such as inhibitors of fatty acid oxidation (FAO), fatty acid transport, and the synthesis
105 of monounsaturated fatty acids [19]. Given the possibility for compensation within lipid
106 metabolic pathways, therapeutic strategies targeting single enzymes are usually met with
107 metabolic adaptations, suggesting combinatorial approaches using established drugs might yield
108 stronger outcomes.
109 In this study, we analyzed the global RNA expression patterns and lipidome of breast
110 cancer cells exhibiting resistance to the three most common ET modalities. Our findings reveal
111 that while the FA composition of ET-resistant cells is distinct from each other and from their ET-
112 sensitive counterparts, they share an increased abundance of LD-storing triglycerides and
113 complex lipids containing polyunsaturated FA (PUFA) species. The FASN inhibitor TVB-2640
114 effectively blocked FASN activity, but variably impacted breast cancer growth. Moreover,
115 certain ET treatments enhanced PUFA levels when FASN was inhibited. These observations

116 continue to establish that ET resistant breast cancer cells develop a distinctive lipid metabolism
117 signature, while emphasizing the complexity of targeting dual FASN and ER activity. Crucially,
118 a reliance on desaturation pathways may represent a novel vulnerability in ET resistance,
119 warranting further investigation.
120
121
122 **Materials and Methods**
123
124 **Generation of Endocrine Therapy Resistant Cell Lines**
125 T47D cells were maintained in minimal Eagle's medium supplemented with 5% fetal bovine
126 serum (FBS), 1x non-essential amino acids (NEAA), 1 nM insulin, and 1 mM sodium pyruvate.
127 The derivation, propagation, generation, and characterization of breast cancer patient-derived
128 xenograft (PDX)- derived cell line, UCD4, was previously described [20]. UCD4 cells were
129 maintained in Dulbecco's Modified Eagle Media/F-12 (50:50) supplemented with 10% FBS, 100
130 ng/mL choleratoxin, and 1 nM insulin. Cell lines were authenticated by short tandem repeat
131 analysis and routinely tested for mycoplasma using the MycoAlert mycoplasma detection kit
132 (Lonza, #LT07-710).
133 T47D and UCD4 cells were exposed to escalating doses of ICI 182780 (Fulv, Faslodex) or 4-
134 hydroxytamoxifen (4OHT, Tam) over a 12-month period to establish endocrine resistance. The
135 starting dose for Fulv and Tam were 10 times lower than the effective dose for each compound, 1
136 nM and 10 nM respectively. Both compounds were dissolved in 100% EtOH to make stock
137 concentrations that resulted in the final cell culture dose being less than 10% EtOH. Fulv
138 resistant (FulvR) and Tam resistant (TamR) cells were maintained at established resistance

139 concentrations, 100 nM and 1 μM, respectively. For estrogen withdrawal, UCD4 cells (UCD4-
140 EWD), were cultured for 12-months in phenol-red free media supplemented with charcoal
141 stripped serum. T47D-EWD cells were derived from T47D cells by serial passage through mice
142 [21] in the absence of estrogen and are maintained in phenol red-free minimal Eagle's medium,
143 5% charcoal stripped FBS, 1x NEAA, 1 nM insulin, 1 mM sodium pyruvate and 2 mM L-
144 glutamine.
145
146 **RNA-sequencing**
147 Parental and resistant cells were plated in 6-well plates at $5x10^5$ (T47D) or $1x10^6$ (UCD4)
148 cells/well in normal media conditions with appropriate maintenance ICI or 4OHT drug
149 concentrations. RNA was isolated using QIAzol lysis reagent (Qiagen, #79306) and RNAeasy
150 Mini Kit (Qiagen, #74104) and treated with RNase-free DNase (Qiagen, #79254). Libraries were
151 prepared by the University of Colorado Genomics Shared Resource using Illumina TruSeq
152 Stranded mRNA Library Prep kit (Illumina, #20020595) and sequenced using paired end 50
153 cycles 2 x 50 on the NovaSEQ 6000 with >30 million reads per sample obtained. Paired-end 150
154 nucleotide reads were aligned to the human genome version GRCh38.p13 using STAR.
155 Downstream expression analysis was performed using Cufflinks. The resulting aligned files
156 (BAM) were then used to infer the differentially expressed gene profiles using DESeq2. Over
157 representation analysis (ORA) was performed using the Gene Ontology (GO) Cellular
158 Component gene set collection via WebGestalt [22].
159
160 **Unbiased Lipid Mass Spectrometry**

161 $1x10^6$ cells were plated in 6 cm plates in normal media conditions (N=4 per condition).
162 Maintenance ICI and 4OHT drug concentrations were added to resistant cell line plates.
163 Modified MTBE liquid-liquid extraction was used with a protein crash. The lipid fraction was
164 reconstituted in 100 µL Methanol. The aqueous fraction was reconstituted in 50 µL 5%
165 Acetonitrile in water. The lipid fraction was run in positive ionization mode on the Agilent 6560
166 IMMS-QTOF, in QTOF-only mode (Analytical column: Agilent Zorbax Rapid Resolution HD
167 (RRHD) SB-C18, 1.8 µm, 2.1x100 mm; column temp 60C; Gradient elution: 0–0.5 minutes 30–
168 70% B, 0.5–7.42 minutes 70–100% B, 7.42–9.9 minutes 100% B, 9.9–10.0 minutes 100–30% B,
169 10–14.6 minutes 30% B; Flow rate 0.6mL/min; Mobile phase A: water with 0.1% formic acid;
170 Mobile phase B: 60:36:4 isopropyl alcohol:acetonitrile:water with 0.1% formic acid) Spectral
171 peaks were extracted using Mass Hunter Profinder version B.08.00 using a Recursive Workflow
172 and area-to-height conversion.
173 The final spectral data were imported into Mass Profiler Professional (MPP) version 14.9
174 Filtered to be present in at least 2 out of the 16 samples. Annotation was performed using our in-
175 house Mass and Retention Time (MSRT) database, HMDB databases, Lipid Maps database,
176 KEGG databases, and a Metiln database. Metaboanalyst and LION were used to generate
177 significant pathways, based on an ANOVA annotated list of compounds. Only pathways with >2
178 compounds in the set were reported.
179
180 **Targeted Lipid Mass Spectrometry**
181 For $^{13}C_2$-acetate tracer studies, $4x10^5$ cells were plated in 6 well plates in normal media
182 conditions (N=3 per condition). Maintenance Fulv and 4OHT drug concentrations were added to
183 resistant cell line plates. Cells were treated with 10 µM TVB-2640 or DMSO for 72 hr. After 24

184 hr of FASN inhibition or vehicle treatment, all wells were supplemented with 250 μM 13C-2
185 acetate for a 48 hr tracer incubation. Cells were harvested with trypsin, pelleted, and flash frozen
186 in liquid nitrogen.
187 Flash frozen cell pellets were lysed in 1ml 66% methanol (vol/vol) in 0.1M potassium phosphate
188 buffer, pH 6.8 by vigorously vortexing twice with 20 second pulses. Reserving 10ul from these
189 lysates, total cellular protein estimation was done using BCA assay (Thermo Fisher, #23225).
190 The remainder of the lysates were then transferred to 13x100mm borosilicate glass culture tubes
191 (Fisher Scientific, #14-961-27). Lysates were acidified with 10ul of 1N HCl (prewashed with
192 Hexanes) and vortexed briefly. Total lipids were extracted twice by adding 1mL of
193 isooctane:ethyl acetate 3:1 (vol/vol) and once with 1mL Hexanes; for each extraction, samples
194 were vortexed vigorously for 10-15 sec and centrifuged at 2000g for 1 minute to complete phase
195 separation. The upper organic layer from each extraction was combined into a new 13x100 mm
196 borosilicate glass tube. Extracted lipids were brought to dryness and resuspend in 300 ul 2,2,4-
197 Trimethylpentane (isooctane). For the non-esterified FA (NEFA) fraction, 100 ul of the
198 resuspended total lipids was transferred to a new borosilicate glass tube, mixed with (30 ng)
199 blended stable isotope internal standard, taken to dryness under gaseous N_2, and resuspended in
200 25ul of 1% pentafluorobenzyl bromide in acetonitrile (vol/vol), to which 25ul of 1%
201 diisopropylethylamine in acetonitrile (vol/vol) was added, and samples were incubated at room
202 temperature for 30 minutes. Pentafluorbenzyl-FA derivatives were taken to dryness under
203 gaseous N_2 and resuspended in 120ul hexanes of injection into the GC/MS. For the total fatty
204 acid fraction (TFA), 20ul of the original 300 uL total lipid extract was transferred to a separate
205 Teflon lined screw cap glass tube, mixed with (66.7 ng) blended stable isotope internal standard,
206 and taken to dryness under gaseous N_2. TFA samples were resuspended in 500 ul of 100%

207 ethanol to which 500 ul of 1M NaOH was added to saponify the TFA fraction at 90C for 30
208 minutes, followed by acidification using 550ul of 1M HCl. Saponified samples were then
209 extracted twice with 1.5ml of Hexanes, taken to dryness under gaseous N_2, and derivatized as
210 above. Derivatized TFA samples were resuspended in 267ul hexanes for injection into the
211 GC/MS. For $^{13}C_2$-acetate tracer samples, 50 ul of the resuspended total lipids was transferred to a
212 new Teflon lined screw cap glass tube, mixed with (66.7 ng) $^{2}D_{31}$-palmitate internal standard and
213 taken to dryness under gaseous N_2. Samples were saponified, extracted, and derivatized as
214 above. Derivatized samples were resuspended in 267ul hexanes for injection. For the NEFA, TFA
215 and tracer fractions, 1ul of pentafluorbenzyl-FA derivatives was injected and data were collected
216 on the GC-MS (8890 GC, 5977B MSD, Agilent) DB-1MS UI column (122-0112UI, Agilent)
217 with the following run program: 80C hold for 3 minutes, 30°C/minute ramp to 125°C, no hold,
218 25C ramp to 320C and hold for 2 minutes. The flow for the methane carrier gas was set at
219 1.5mL/minute. Data were acquired in full scan negative chemical ionization mode to identify
220 fatty acids of acyl chain length from 8 to 22 carbons. Peak areas of the analyte or of the standard
221 were measured, and the ratio of the area from the analyte-derived ion to that from the internal
222 standard was calculated [23]. $^{13}C_2$-acetate tracer incorporation into palmitic acid was analyzed in
223 two carbon increments from M+2 (257 m/z) to M+16 (271 m/z) relative to the quantitative $^{2}D_{31}$-
224 palmitate internal standard [24-26].
225
226 **Oil Red O Staining**
227 500 mg of Oil Red O (ORO) powder was dissolved in 10 mL of 100% propylene glycol (PEG).
228 While heating ORO/PEG solution in 95C bead bath 90 mL of 100% PEG was added to solution
229 in 10 mL increments with vigorous swirling in between additions. Once ORO/PEG solution

230 cooled to room temperature and before each use, solution was filtered using a Whatman #4 filter
231 paper. For 2D culture: 18mm glass coverslips were sterilized in 100% ethanol overnight and
232 placed in 6-well plates. Parental and ET resistant T47D or UCD4 cells were plated on glass
233 coverslips at $5x10^4$ cells/well in normal media conditions with appropriate maintenance Fulv or
234 4-OHTam drug concentrations. Cells were cultured for 5 days at 37C and 5% CO_2 without
235 refreshing medium. After 5 days, cells on coverslips were washed three times with PBS and
236 fixed in 10% buffered formalin for 10 minutes. Formalin was aspirated followed with three more
237 washes of PBS. 1mL of 100% PEG was added per well for 2 minutes then aspirated to waste. 1
238 mL of ORO/PEG solution was added to each well and incubated for 15 minutes. ORO/PEG
239 solution was removed to waste, and wells were washed with 60% PEG for 2 minutes. Wells were
240 rinsed with DI H_2O three times and counterstained with 1mL diluted 1:50 Harris Hematoxylin
241 (Fisher Scientific, #SH30-4D) for 10 minutes. Hematoxylin was discarded and wells were
242 washed with DI H_2O until clear. Cells on coverslips were mounted on Fisherbrand™
243 ColorFrost™ Plus Microscope Slides (Fisher Scientific,#12-550-17) using tweezers and aqueous
244 mounting medium (Electron Microscopy Sciences, #17985-10). All slides were imaged at 20X
245 magnification (Olympus, BX40). Neutral lipid stain was quantified on ImageJ and normalized to
246 cell area (4 fields per condition).
247
248 **Immunoblots**
249 All cell lysates for immunoblotting were harvested in RIPA buffer. 100 mg total protein per
250 sample were separated on 7.5% SDS-PAGE gels. Primary antibodies were as follows: FASN
251 (rabbit #3180, Cell Signaling Technologies, 1:1000), ACC1(rabbit #3676, Cell Signaling
252 Technologies, 1:1000), or β-actin (mouse A5441, Sigma, 1:2000). Secondary antibodies were

253 IRDye800CW goat-anti-mouse IgG (926-32210, LiCor Biosciences) and IRDye 680LT goat-
254 anti-rabbit IgG (926-68021, Li-Cor Biosciences) both at 1:5,000. Immunoblots were imaged and
255 analyzed with the Odyssey Infrared Imaging System and Image Studio Lite (LiCor Biosciences).
256
257 **Cell proliferation**
258 Real-time imaging (IncuCyte, Sartorius, Ann Arbor, MI) was used to measure proliferation of
259 cells at × 10 magnification. UCD4 cells were plated at 15,000 cells/well, T47D cells at 20,000
260 cells/well, sextuplicate samples in 96-well plates. For treatments, cells were given vehicle, 10
261 μM TVB-2640 plus 1 μM 4OH-Tam, or 100 nM Fulv on day one. Cells were counted under
262 phase contrast immediately after treatment and subsequently taken every 4 h for 6 days. Counts
263 were calculated as fold change over time zero. Significance was assessed by two-way repeated
264 measures ANOVA for growth curves and t-tests for individual time points.
265
266 **Statistical Analyses.** Statistical analyses were performed with GraphPad Prism 10. Data were
267 plotted as means ± SEM. Two-tailed $p < 0.05$ was considered statistically significant. Asterisks
268 denote levels of statistical significance as determined by one or two-way ANOVA with Tukey's
269 or Dunnett's multiple comparisons test, unpaired two-tailed t-test, one-sided Fisher's exact test,
270 log- rank Mantel-Cox test, Wilcoxon rank sum test, or Chi-squared test for trend. Specific tests
271 used are indicated in the figure legends. All experiments were performed in minimum triplicate
272 biological replicates unless noted otherwise.

Results

Lipid metabolic pathways are upregulated with ET resistance

ET resistant variants of T47D and UCD4 cells were generated by escalating the dose of 4-hydroxytamoxifen (1 μM, TamR), or Fulvestrant (100 nM, FulvR), or by placing cells in estrogen withdrawal/deprivation media (EWD, phenol red free, dextran charcoal stripped), for 6 months. We assessed transcriptional changes that associated with ET resistance by conducting RNA-sequencing on UCD4 parental and ET resistant (EWD, TamR, FulvR) cell lines. Principle component analysis of the UCD4 cells indicates that EWD, TamR, and FulvR have broad differences in their gene expression that make them distinct from each other (**Figure 1a**). Differentially expressed genes (DEG; $\geq$ 2-fold change, FDR<0.05) were calculated within each of the UCD4 ET resistant groups relative to the parental line, identifying 918, 1,293, and 1,042 total DEG in the EWD, TamR, and FulvR vs parental lines respectively (**Figure 1b**). In common among the DEG lists across UCD4 ET resistant lines were 467 genes, while 92 were shared between EWD and FulvR, 347 were shared between FulvR and TamR, and 150 DEGs were shared between EWD and TamR (**Figure 1c**). Gene Ontology (GO) analysis for the Biological Processes category calculated the top 10 significantly enriched terms associated with each DEG list (**Figure 1d**), which identified lipid metabolism and lipid associated processes as a common feature among the three ET-resistant cell lines. ET resistant cell lines had reduced proliferation rates compared to the parental lines (**Figure S1a-b**). ER expression is lost in T47D-EWD and reduced in FulvR but not TamR cells, while UCD4 ET resistant cell lines all retained ER expression (**Figure S1c)**.

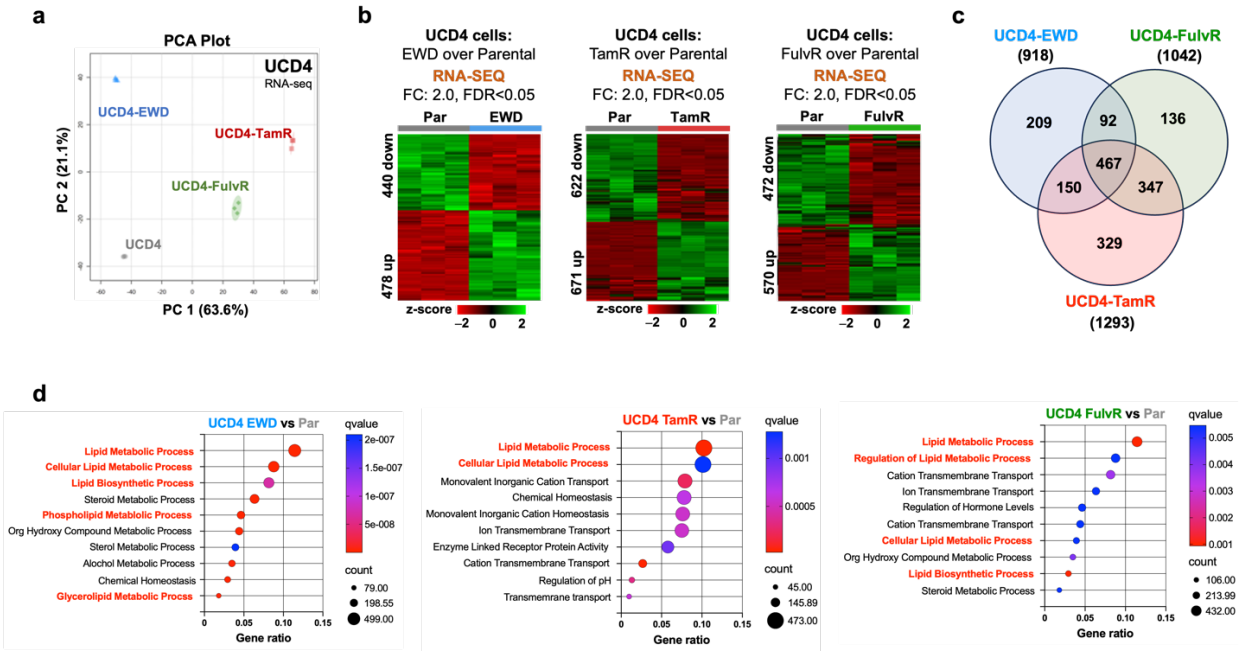

Figure 1: Lipid metabolic pathways are upregulated in endocrine resistant breast cancer cells.

a) Principal component analysis (PCA) plots of UCD4 parental and ET resistant (TamR, FulvR, EWD) cell RNA-sequencing data. Triplicate samples.

b) Heatmaps of significantly upregulated and downregulated genes between UCD4 parental and ET resistant cell samples. A fold change (FC) cutoff of 2.0 and False discovery rate (FDR) less than 0.05 was used.

c) Venn diagram of overlapping significantly altered transcripts of UCD4 ET resistant versus parental cells.

d) Over representation analysis plots of UCD4 ET resistant cell gene enrichment analysis using Gene Ontology (GO) Biological processes gene sets. Top 10 significantly upregulated pathways indicated.

309

310 **The global lipidome is altered in ET resistant breast cancer cells**

311 Unbiased lipid mass spectrometry was used to identify changes associated with ET
312 resistance in both the T47D and UCD4 parental lines, as well as the derived EWD, TamR, and
313 FulvR cell lines. Much like the gene expression profiling, PCA analysis of lipidome data indicate
314 samples distinctly cluster according to parental or ET resistant type (**Figure 2a-b**). Using the
315 publicly available metabolomics analysis tool Metaboanalyst, we found the top 25 significantly
316 different analytes between ET resistant variant and its parental sample, including various
317 phospholipid (PE, PC, PI, PA), glycerolipid (TG, DG), and cholesterol species (**Figure 2c-d**). To
318 identify differential lipids that are in common or unique among ET resistant lines, we compared
319 all significantly altered analytes from each ET resistant compared to parental cell lines (**Figure**
320 **2e-f**). T47D ET resistant samples shared 321 overlapping analytes while there were 128
321 overlapping analytes in UCD4 ET resistant cell lines. We then characterized the overlapping
322 analytes by lipid class and found that most altered lipid species with ET resistance in both T47D
323 and UCD4 cells were phosphatidylcholine (14% and 26.7%), phosphatidylethanolamine (12.4%
324 and 15.6%), and triglyceride (12.8% and 18.8%) species (**Figure 2g-h**).

325

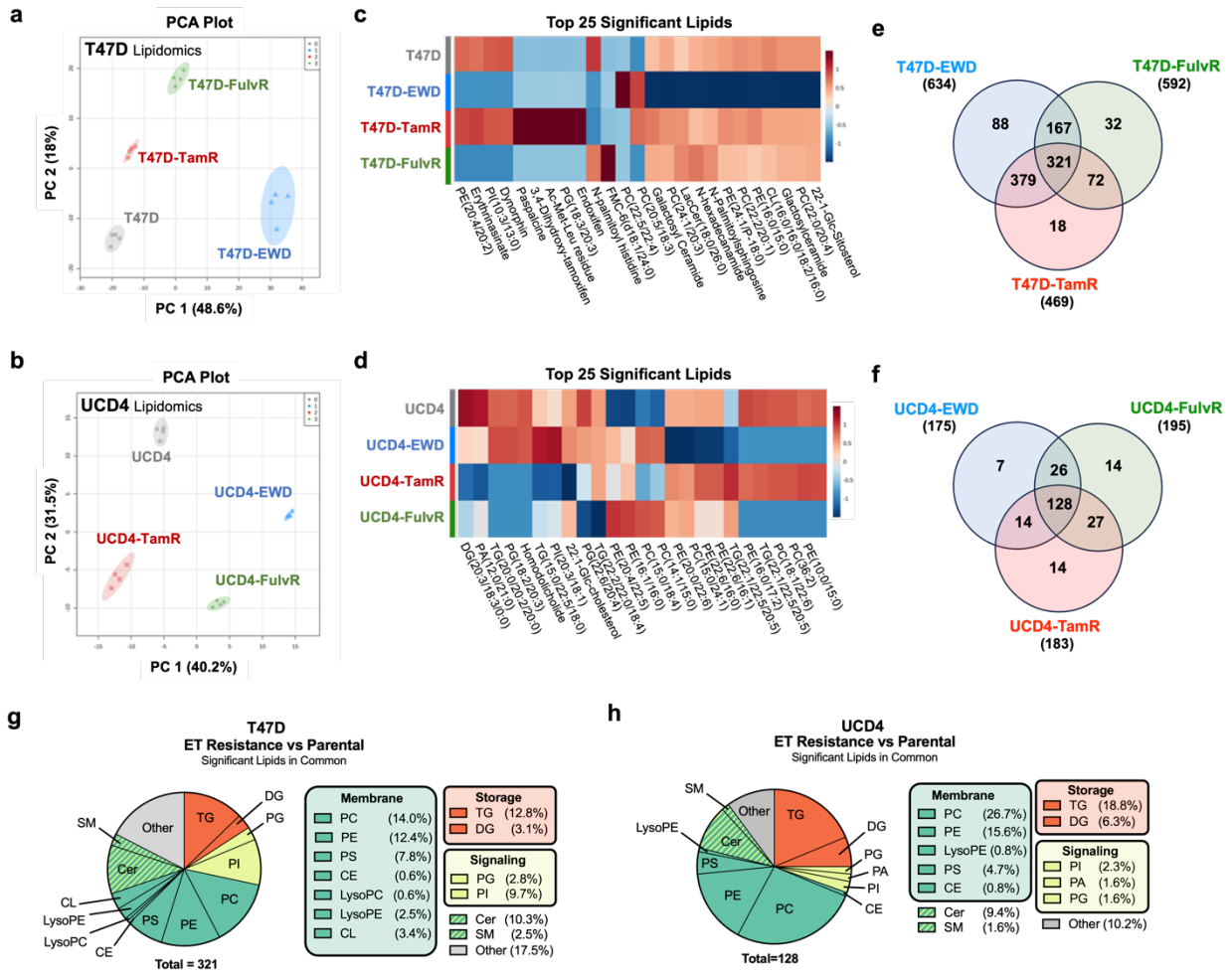

Figure 2: The global lipidome is shifted in endocrine resistant breast cancer cells.
a-b) Principal component analysis (PCA) plots of T47D (a) and UCD4 (b) parental and ET resistant cell samples profiled by lipidomics.
c-d) Heatmap of top 25 significantly altered lipid analytes between T47D (a) and UCD4 (b) parental and ET resistant cell samples by ANOVA analysis using Metaboanalyst.
e-f) Significantly altered lipid analytes from T47D (e) and UCD4 (f) parental cells compared among the ET resistant cells.
g-h) Pie charts of shared significantly altered lipid analytes compared to parental cells across all ET resistant T47D or UCD4 cells.

336 To evaluate the potential function of the observed global lipidome changes, we used
337 Lipid Ontology (LION), a publicly available resource that groups analytes within lipidomic data
338 sets by lipid class and function [27]. LION-PCA heatmap analyses on T47D and UCD4 ET
339 resistant compared to parental cells clustered significant analytes into lipid signatures (**Figure**
340 **S2a-b**). The lipid signature containing neutral storage lipids was the most consistently
341 upregulated among ET resistant sublines (2/3) in both T47D and UCD4 cell lines (**Figure 3a-b**).
342 Lipid categories including PUFAs and FAs with double bonds were also upregulated in some ET
343 resistant cell lines suggestive of a trend in ET resistance. Overall, these analyses identify a
344 significant alteration in the global lipidome associated with ET resistance.
345

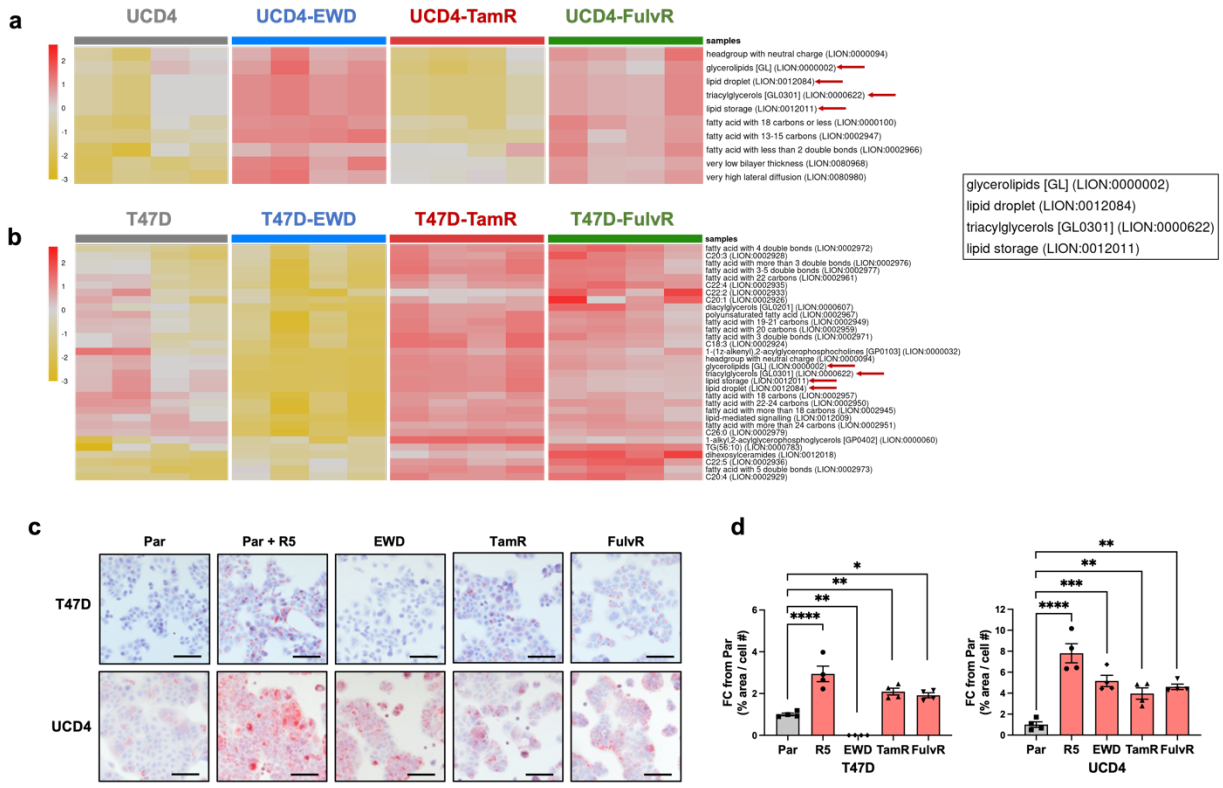

Figure 3: ET resistant breast cancer cells increase cytoplasmic lipid storage.
a-b) Lipid storage LION-signature by hierarchical clustering. LION-PCA heatmap analysis of UCD4 (a) and T47D (b) parental and ET resistant cell lipidomics data. Heatmap colors (from yellow to red) indicate the mean z-score. Names and IDs of the selected terms are displayed on the right. Samples are sorted by sample group.
c) Oil Red O staining of T47D and UCD4 parental and ET resistant cells. 5 x 10^4 cells were plated on glass coverslips in normal media conditions (n=4 each). Positive control cells were treated with 10nM promegestone (R5) for 5 days. Cells were formalin fixed, stained with ORO, counterstained with diluted hematoxylin, mounted on slides, and imaged by light microscopy at 40X.
d) Quantification of ORO staining. Images were quantified by ImageJ software (4 fields per condition). One-way ANOVA statistical comparison was used to compare ORO staining in ET resistant to parental cells. *P<0.05; **P<0.01; ***P<0.0001; ****P<0.0001.

361

362 **Lipid storage is enhanced during endocrine resistance**

363 Since triglycerides were increased in most T47D and UCD4 ET resistant cell lines and
364 lipid storage was a feature identified by LION analyses, we conducted Oil Red O (ORO) neutral
365 lipid staining on our collection of cell lines to visualize intracellular lipids (**Figure 3c**). A
366 synthetic progestin (R5020) was used as a positive control for inducing LD formation [8]. Both
367 T47D and UCD4 parental cell lines displayed basal positive staining for lipid storage which was
368 visibly enhanced with R5020 treatment. All ET resistant cells with the exception of T47D-EWD
369 showed significantly increased LD staining compared to parental controls (**Figure 3d**). T47D-
370 EWD cells are unique in that they transition to a basal-like phenotype and lose expression of ER
371 and progesterone receptor, PR [28]. To test whether T47D-EWD compared to other ET resistant
372 cells were using FAO, a Seahorse Palmitate Oxidation FAO assay was run across all cell lines
373 (**Figure S3**). No significant use of FAO was detected in T47D or UCD4 Par or ET resistant cells.

374

375 **FASN catalysis is not required for ET resistant breast cancer cell proliferation**

376 Enhanced lipid storage can be indicative of increased FA abundance either through the *de*
377 *novo* biosynthesis pathway and/or through FA uptake. We assessed levels of the two rate limiting
378 enzymes in de novo FA synthesis, FASN and ACC1, by immunoblot (**Figure 4a & S4**). FASN
379 expression was elevated or unchanged in ET resistant compared to parental cell lines, except for
380 UCD4-TamR where FASN levels decreased. ACC1 was also elevated or unchanged in ET
381 resistant cell lines compared to parental. Additionally, we confirmed there were no significant
382 changes in ACC1 phosphorylation between parental and ET resistant cells, suggesting ACC1 is
383 maintained in an active state during ET resistance (**Figure S4**). To assess FASN activity, we used

384 $^{13}C_2$-acetate stable isotope tracing and lipid mass spectrometry to quantify the amount of isotope
385 incorporated palmitate (C16), the primary product of FASN, in T47D-Par, Par plus R5020,
386 TamR, and FulvR cells (**Figure 4b**) in the absence or presence of the FASN inhibitor TVB-2640.
387 R5020 treated parental (positive control), TamR, and FulvR cells compared to vehicle treated
388 parental cells had significantly higher isotope incorporation, suggesting ET resistance elevates
389 FASN enzymatic activity. Addition of TVB-2640 ablated isotope incorporation into palmitate in
390 both T47D-Par, Par plus R5020, -TamR and -FulvR cells, validating its potency at FASN
391 enzymatic inhibition.
392 To test whether FASN inhibition affected lipid accumulation, we used ORO staining in
393 parental and ET resistant cells plus or minus TVB-2640. Treatment with TVB-2640 was
394 sufficient to block progestin-induced LD formation in T47D and UCD4 parental cells (**Figure**
395 **4c-d**). Mixed results were observed between ET resistant cells. Within T47D cell lines, TVB-
396 2640 reduced LDs in T47D-TamR cells, and increased their abundance in T47D-FulvR cells and
397 LD deficient T47D-EWD cells. TVB-2640 was sufficient to reduce LDs in all ET resistant
398 UCD4 cell lines, and increased their levels in UCD4-Par cells.
399

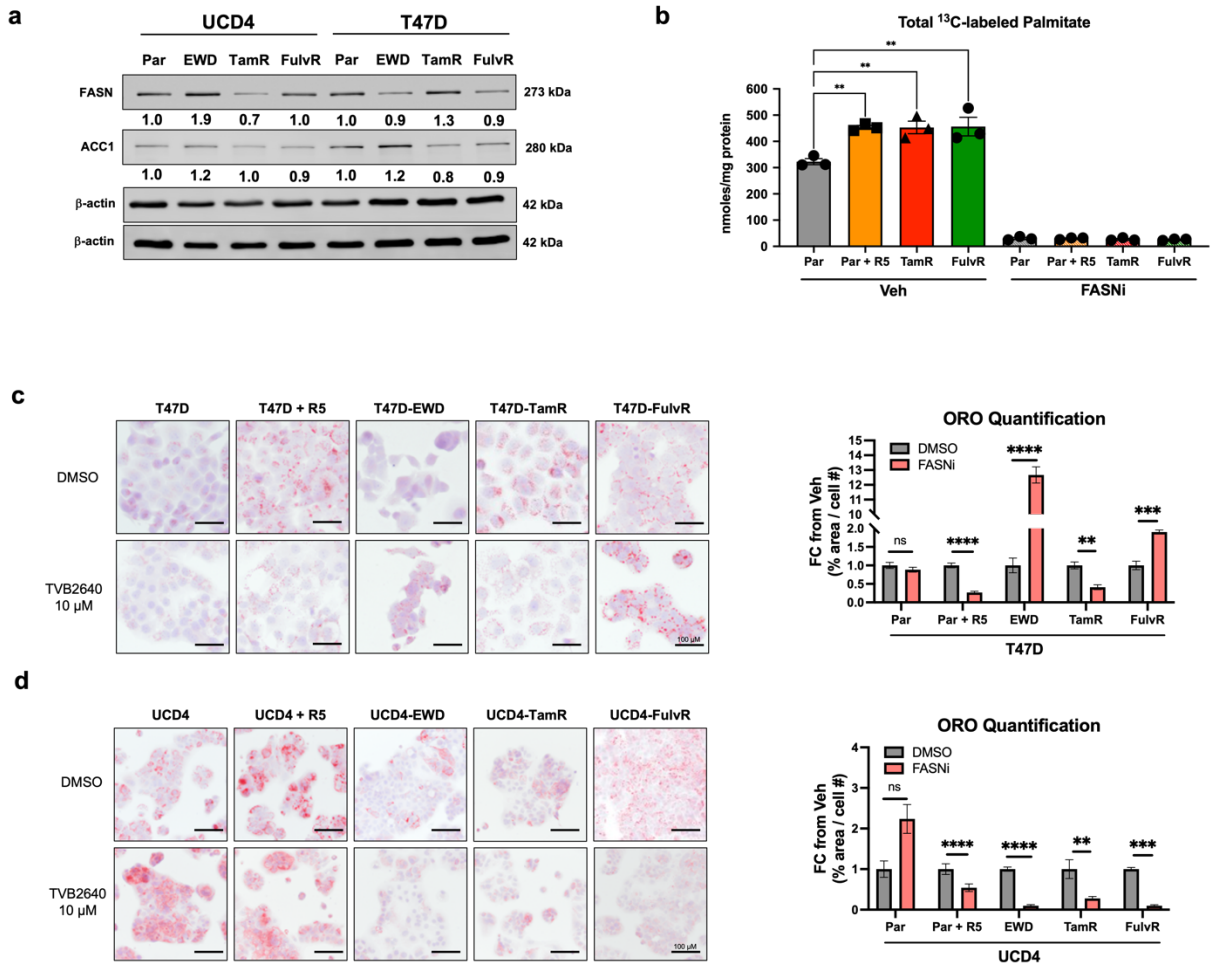

Figure 4: FASN activity is elevated in ET resistant breast cancer cells and drives altered lipid morphology.

a) Immunoblot analysis of FASN and ACC1 from parental and ET resistant T47D and UCD4 cells. Bands were normalized to β-actin and fold change over parental is indicated.

b) Quantification of $^{13}C_2$ acetate tracer incorporated into palmitate from T47D parental and ET resistant cells. Cells were treated with veh (DMSO) or 10uM TVB-2640 for 72 hrs.

c-d) ORO staining and quantification of T47D(c) and UCD4 (d) parental and ET resistant cells with or without TVB-2640 treatment. 15 x 10^3 parental and ET resistant cells were plated on glass coverslips in their normal media conditions (in the presence of drugs where appropriate). Cells were treated with vehicle (DMSO) or TVB-2640 (10uM) for 5 days. Positive control cells were treated with 10nM promegestone (R5) plus/minus 10 μM TVB-2640 for 5 days. Cells were formalin fixed, stained with ORO and diluted hematoxylin, mounted on slides, and imaged using an Olympus BX40 microscope. Scale bars, μm. *P<0.05; **P<0.01; ***P<0.0001; ****P<0.0001.

416 Since FASN activity could be effectively ablated with TVB-2640, we assessed the impact
417 of the inhibitor on the proliferation of ET resistant cells. Parental and ET resistant cells were
418 treated with TVB-2640 at the equivalent dose to tracing studies (10 μM) and monitored using
419 Incucyte live cell analysis (**Figure 5**). T47D and UCD4 Par and ET resistant variants showed
420 minimal differences in proliferation between vehicle and TVB-2640 treated cells at 72 h, the
421 timepoint used for tracing studies (**Figure 5a-b**). However, by 6 days post-treatment T47D cells
422 showed significant >1.5 fold change reduction in proliferation. UCD4 cell proliferation was not
423 significantly impacted by TVB-2640 across 6 days of treatment (**Figure 5c-d**). To assess whether
424 higher doses could have more potency on cell growth, we performed IC50 analyses in T47D and
425 UCD4 parental and ET resistant cells (**Figure S5**). T47D cells had IC50 values between 9-18
426 mM. UCD4 cell lines did not achieve efficient cytotoxicity at the highest solvent dose and IC50
427 ranges could not be determined. Thus, the FASN inhibitor TVB-2640 effectively reduced FASN
428 activity, had a variable impact on LD storage; these parameters did not correlate, however, with
429 significant growth reduction.

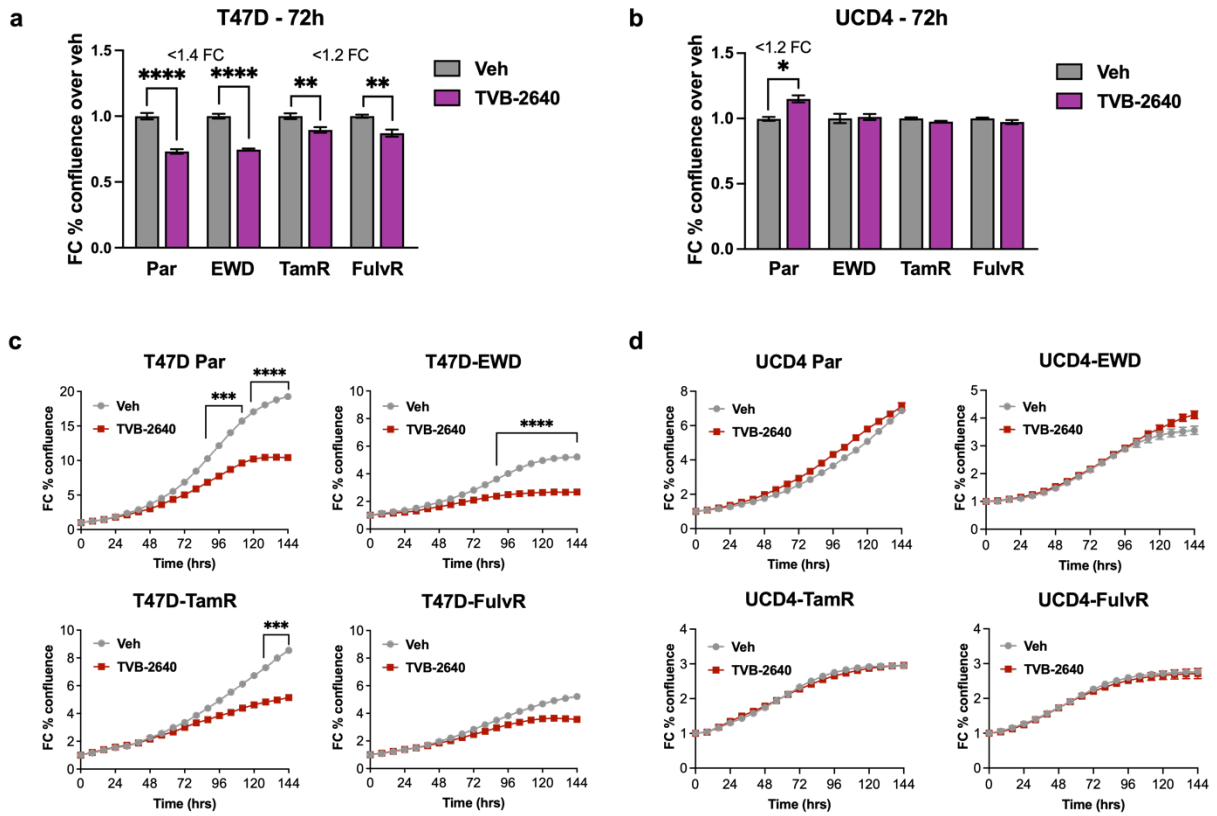

Figure 5: FASN inhibition is not sufficient to target ET resistance.
a-b) 72 hr timepoint percent confluence fold change (FC) bar graphs of T47D (a) and UCD4 (b) parental and ET resistant cells treated with 10uM TVB-2640 or vehicle (Veh). FC is indicated where significant by t-test comparing treatment to veh; *P<0.05; **P<0.01; ****P<0.0001. c-d) Proliferation growth curves of T47D (c) and UCD4 (d) parental and ET resistant cells treated with 10uM TVB2640. Fold change (FC) from timepoint 0 was calculated using Incucyte. Two-way ANOVA significance was calculated and is indicated for timepoints with ≥1.5 FC. ***P<0.0001; ****P<0.0001.

439 **ET resistance increases lipids with unsaturated acyl chains**

440 LION enrichment analysis implicated higher abundance of lipids with increased
441 desaturation (**Figure S2**). This was particularly notable in T47D ET resistant cells, with the top
442 10 altered LION pathways including complex lipids with FAs containing > 3 double bonds
443 (**Figure 6a**). To assess this in more detail, lipids detected by lipidomics were stratified by degree
444 of unsaturation (number of double bonds) (**Figure 6b**). Both T47D and UCD4 ET resistant
445 compared to parental cells have a higher level of complex lipids with 9 or more double bonds,
446 with T47D cells showing a larger change. The dataset was further queried to determine which
447 lipid classes harbored PUFA acyl chains. Most lipid species with >6 double bonds aligned to
448 triglycerides and phospholipids suggesting lipids with PUFA acyl chains are distributed between
449 the membrane and/or sequestered in LDs (**Figure 6c**).

450 To further investigate PUFA abundance in ET resistant compared to parental cells, we
451 analyzed their levels in T47D parental and ET resistant cells from tracing studies, where acyl
452 chains were chemically liberated. Long chain (LC)-PUFAs, including arachidonic acid (AA),
453 eicosapentaeonic acid (EPA), and docosahexanoic acid (DHA), increased in T47D-TamR and
454 FulvR compared to parental cells (**Figure 6d**). Interestingly, FASN inhibition with TVB-2640
455 increased LC-PUFAs specifically in T47D-FulvR cells, which have increased lipid accumulation
456 with drug treatment (**Figure 4c-d**). We further assessed levels of n-6 (including AA) and n-3
457 PUFAs (including EPA, DHA) PUFAs (**Figure 6e-f**). Both n-6 and n-3 PUFAs were elevated in
458 T47D-TamR and -FulvR compared to parental cells. Again, TVB-2640 treatment increased n-3
459 and n-6 PUFAs in T47D-FulvR cells. No differences in LC, n-6 or n-3, PUFAs were observed
460 with progestin (R5020) treatment in the absence or presence of TVB-2640, suggesting elevated
461 PUFA synthesis is a feature specific to ET resistant breast cancer cells. Together these data

462 demonstrate that LC-PUFAs are specifically increased in ET resistant compared to parental cells
463 implicating desaturase activity as an alternate lipid metabolism target in drug resistant breast
464 cancer.
465

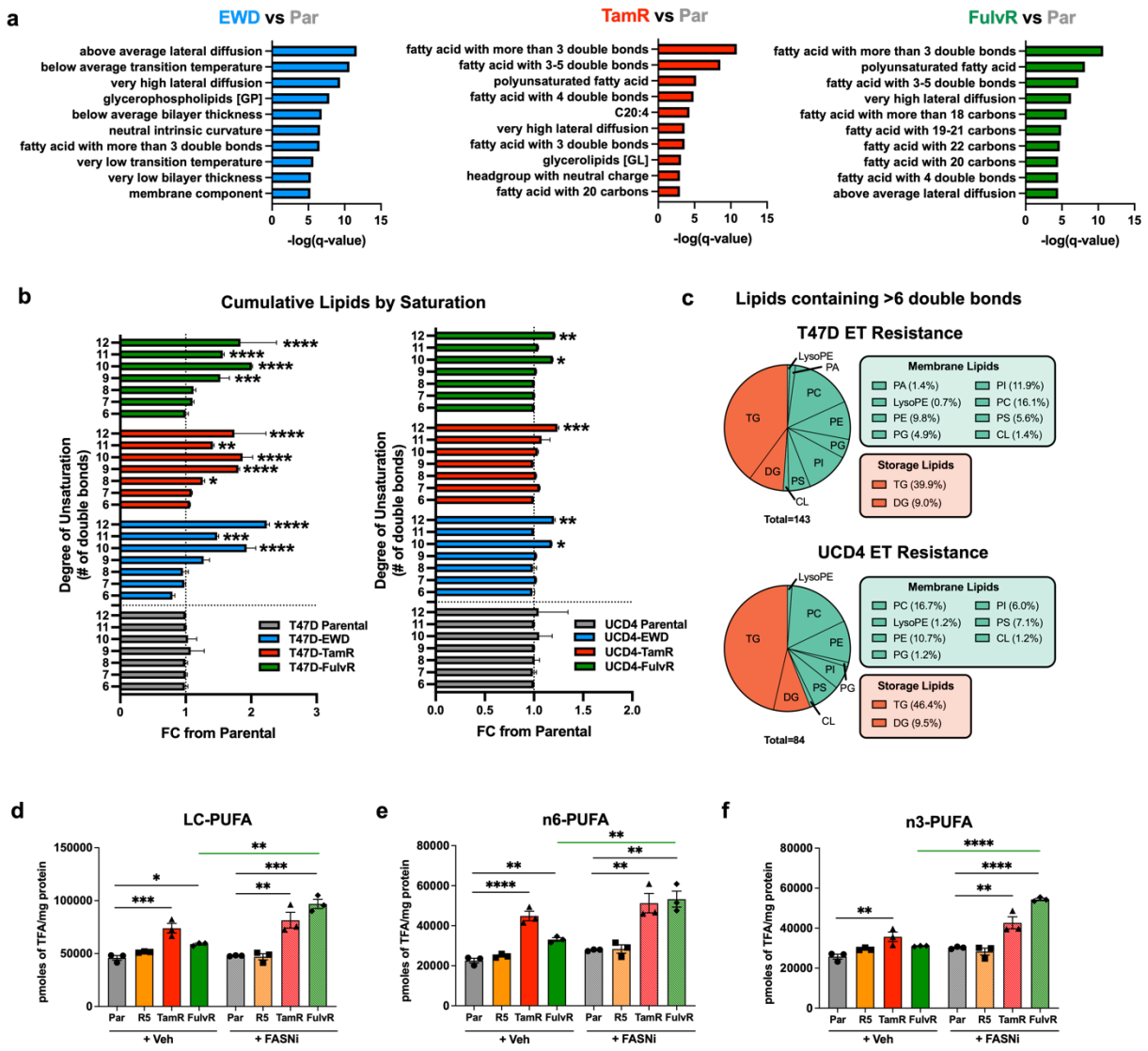

Figure 6: Endocrine resistant breast cancer cells enhance lipids with unsaturated acyl chains.

a) LION enrichment plots of T47D ET resistant versus parental cell lipidomics.

b) Graphs of cumulative lipid analytes from T47D (left) and UCD4 (right) ET resistant and parental cells by degree of lipid saturation (6 or more double bonds). One-way ANOVA compared to parental; *P<0.05; **P<0.01; ***P<0.0001; ****P<0.0001.

c) Pie charts of lipids containing polyunsaturated fatty acids (PUFAs) with 6 or more double bonds by lipid class.

d-f) Total 2-13C-acetate tracer incorporated long chain (e), n6 (f), and n3 (g) PUFAs in T47D ET resistant and parental cells treated with veh (DMSO) or FASN inhibitor (10 uM TVB2640, 72 hr). One-way ANOVA comparing ET resistant to parental T47D cells plus/minus vehicle (Veh) or TVB-2640 FASN inhibitor (FASNi). T-test comparing each treatment plus/minus FASN inhibitor. *P<0.05; **P<0.01; ***P<0.0001; ****P<0.0001.

481 **Discussion**

482

483 Lipid metabolic reprogramming is a hallmark of breast cancer and evidence supports this
484 differs among the breast cancer subtypes [29]. In this study, we focused on aberrant lipid
485 metabolism in ER+HER2− breast cancer during acquisition of ET resistance (**Figure 7**). We
486 identified that breast cancer cells resistant to several forms of ET versus their sensitive
487 counterparts commonly increase lipid storage and their lipidomes contain more PUFAs. Our data
488 indicate that ET resistant cells increase both de novo FA synthesis and processing of exogenous
489 FAs into LC-PUFAs. Here we speculate that breast cancer cells adapt to chronic endocrine
490 disruption by activating multimodal FA synthesis and processing pathways and that targeting
491 synthesis alone is unlikely to be effective in ER+ ET resistant breast cancer.

492 LD accumulation is considered a common feature of aggressive cancers although their
493 precise role in tumor progression is unknown [30]. LDs are organelle-like structures that are
494 synthesized in the endoplasmic reticulum and mainly composed of neutral lipid triglycerides and
495 cholesterol esters. These LDs can supply triglycerides for energy reserves, membrane synthesis,
496 and signaling. One proposed novel role for LDs in aggressive cancers is the sequestration of
497 drugs. Schlaepfer et al demonstrated that progestins increase LDs in breast cancer cells and that
498 these LDs can sequester taxanes [8]. We speculate that LDs may also sequester Tam and Fulv in
499 ET resistant cells as they are fat soluble molecules. TamR breast cancer cells have previously
500 been observed to increase LDs [13]. Our studies demonstrate that resistance to Tam, Fulv, and
501 EWD are all accompanied by exacerbated lipid storage. Thus, increased LD production may be a
502 common stress adaptation to chronic endocrine disruption. One exception is T47D-EWD cells
503 which have a notable decrease in LDs. These cells are unique in that they lose expression of ER

504 and PR and transition to a basal TNBC phenotype [21]. TNBC cells are relatively more reliant on
505 FAO [31]. Ahn et al demonstrated that TamR cells have an increased FAO gene signature
506 associated with TNBC [32]. Our studies utilizing Seahorse FAO assays did not detect increased
507 FAO in any of our ET resistant cells including T47D-EWD. FASN inhibition had a variable
508 impact on LD abundance in ET resistant cells, implicating that these structures have more
509 complex roles in FA metabolism and drug resistance.

510 It is well recognized that breast cancer versus normal cells increase FASN driven de novo
511 FA synthesis [6]. FASN is a long-studied lipid metabolism target as it is universally increased in
512 breast carcinoma cells and linked to worse prognosis [16, 33, 34]. Most preclinical studies have
513 found FASN blockade synergizes with chemotherapy drugs [17]. However, investigation of
514 FASN inhibition in the context of ET resistance is limited. TVB compounds are reversible
515 imidazopyridine-derived inhibitors of FASN. Since ET resistant cells have elevated FASN levels
516 in tandem with increased lipid storage, we tested how the new generation FASN inhibitor TVB-
517 2640 impacted ET resistant cells. While TVB-2640 effectively decreases FASN activity
518 demonstrated by lack of palmitate synthesis, it had a variable effect on LD abundance in treated
519 cells. In particular,T47D-EWD and -FulvR cells increased LDs with FASN blockade. In T47D-
520 FulvR cells we noted FASN inhibition increases PUFAs. This suggests that some cells may react
521 to blockade of de novo synthesis by uptaking essential FAs and processing them into LC-PUFAs.
522 FASN blockade reduced the growth of all T47D cell lines at late (5-6 days) but not early (3 days)
523 time points, indicating a delayed effect, and one that does not coincide with LDs. TVB-2640
524 treatment reduced LDs in all UCD4 ET resistant cells. Interestingly, growth of UCD4 cells was
525 unaffected by TVB-2640, suggesting cells are not reliant on FASN activity and LDs for their
526 drug resistance. LDs alone are therefore not a reliable read-out of FASN activity. Both the Phase

527 I trial of TVB-2640 and the ongoing Phase II trial (prioritizing advanced HER2+ breast cancers)
528 are in combination with chemotherapy (NCT03179904). Malonyl carnitine, a metabolite of
529 malonyl-CoA, increased in the serum of patients taking TVB-2640, demonstrating in vivo target
530 efficiency [18]. The efficacy of TVB drugs in combination with ET, despite effective FASN
531 blockade, may have other off target activities. For example, Gruslova et al demonstrated that the
532 closely related FASN inhibitor TVB-3166 decreased growth of TamR MCF7 cells potentially
533 through degradation of ER [12]. Our data insinuate that blocking de novo FA synthesis in ET
534 resistant breast cancer cells may not be sufficient to improve treatment due to well recognized
535 lipid metabolic flexibilities. A recent study found that inhibiting ACC1 to block malonyl-coA
536 synthesis could resensitize long term estrogen deprived breast cancer cells in some contexts,
537 prospectively by blocking peroxisome mediated LC-FA oxidation (REF)..

538 Our experiments uncovered that ET resistant versus parental cells contain a higher
539 content of lipids with increased degrees of unsaturation, particularly PUFAs with greater than
540 nine double bonds. Interestingly, in T47D-FulvR cells, PUFAs increased further upon FASN
541 inhibition. PUFAs provide building blocks for membrane expansion and their synthesis provides
542 energy in the form of NADPH for other metabolic reactions. However, excessive storage of
543 PUFAs leaves cells vulnerable to lipid peroxidation, which can trigger cell death through
544 processes such as ferroptosis [35]. The enzymes that catalyze the generation of double carbon
545 bonds in FAs are the FA desaturases (FADS). The main FADS in humans include FADS5,
546 otherwise known as Stearoyl-CoA Desaturase (SCD), which produces monounsaturated FAs
547 from C16 and C18 FAs, and FADS1, FADS2, that produce n-6 and n-3 PUFAs from the essential
548 C18 FAs linolenic acid and α-linolenic acid, respectively [36]. While most studies have focused
549 on inhibiting SCD, several recent studies have focused on blocking other FADS in cancer. Vriens

550 et al identified that by inhibiting SCD in breast cancer cells (not ET resistant), FADS2
551 compensates by producing the alternative FA sapienate, and FADS2 inhibition could reverse this
552 process [33]. Thus, disrupting PUFA synthesis by FADS could be particularly damaging to ET
553 resistant cells. We observed other lipid metabolic changes in ET resistant cells such as altered
554 membrane lipid content that could also reveal vulnerabilities in ET resistance and will require
555 further investigation.
556

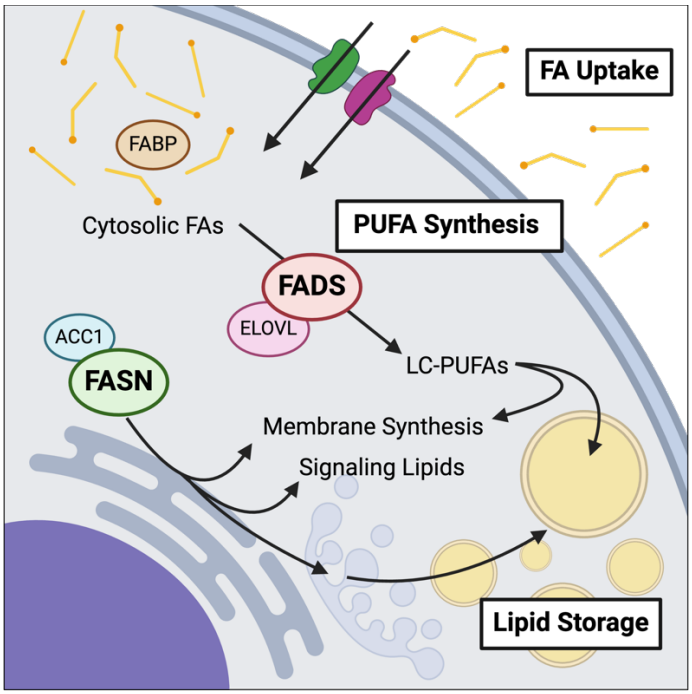

Figure 7: Overview of upregulated lipid biology in ET resistance.
ACC1: acetyl-CoA carboxylase 1; ELOVL: Fatty Acid Elongase; FABP: fatty acid binding protein; FADS: fatty acid desaturase; FA: fatty acid; FASN: fatty acid synthase; LC-PUFA: long-chain poly unsaturated fatty acid.

565 **Conclusions**

566 We demonstrate that breast cancer cells resistant to ET have increased FASN activity, PUFAs,
567 and lipid storage. Targeting de novo synthesis in the presence of ET drugs selectively impacted
568 cell growth and did not correlate with LD reduction, suggesting ET resistant breast cancer cells
569 may evade FASN inhibition through other lipid metabolic pathways including exogenous uptake.
570 This prospectively includes the uptake of essential PUFAs that undergo further elongation and
571 desaturation events and may present a unique vulnerability for targeting desaturation in ET
572 resistant breast cancer cells.

573

574 **Abbreviations**

575 ACC: Acetyl CoA carboxylase

576 ER: Estrogen Receptor alpha

577 ET: Endocrine therapy

578 EWD: Estrogen withdrawal

579 FA: Fatty acid

580 FADS2: Fatty Acid Desaturase 2

581 FASN: Fatty acid synthase

582 FAO: Fatty acid oxidation

583 Fulv: Fulvestrant

584 FulvR: Fulvestrant resistant

585 PUFA: Polyunsaturated fatty acid

586 LC-PUFA: Long chain polyunsaturated fatty acid

587 LD: Lipid droplet

588 ORO: Oil Red O

589 PR: Progesterone receptor

590 SERD: Selective estrogen receptor modulator degrader?

591 SERM: Selective estrogen receptor degrader modulator?

592 SREBP1: sterol regulatory element-binding transcription factor 1

593 Tam: Tamoxifen

594 TamR: Tamoxifen resistant

595 TNBC: Triple negative breast cancer

596

597 **Declarations**

598

599 **Ethics approval and consent to participate**

600 All animal procedures were approved by the Colorado Institutional Animal Care and Use

601 Committee.

602

603 **Acknowledgements**

604 We thank the University of Colorado School of Pharmacy Mass Spectrometry Facility for their

605 consultation and services. We thank the University of Colorado Cancer Center Genomics, Cell

606 Technologies, and Pathology Shared Resources supported by P30CA046934.

607

608 **Author contributions**

609 A.V.W, P.K., M.C.R., and C.A.S. designed the studies. R.R.V., K.B.H., and M.C.R. conducted

610 lipidomic and tracing studies. A.V.W. and D.R. conducted cell culture based experiments. A.V.W,

611 D.R., R.R.V., M.C.R. and C.A.S. conducted all data analysis. A.V.W. and C.A.S. drafted
612 manuscript. D.R., J.F.S, H.M.B., R.R.V., P.K., and M.C.R. reviewed and edited manuscript.
613 Project was supervised and funded by M.C.R. and C.A.S. All authors have read and agreed to the
614 published version of the manuscript.
615
616 **Funding**
617 This work was supported by National Cancer Institute grants R01CA140985 (C.A.S.) and
618 1F31CA261053 (A.V.W.), the Breast Cancer Research Foundation 23-144 (C.A.S.), the Cancer
619 League of Colorado (C.A.S, A.V.W.)
620
621 **Availability of data and materials**
622 The raw RNA-sequencing data is available in the NCBI Gene Expression Omnibus (GEO
623 Accession XXX). The unique cell lines are available to qualified individuals for research
624 purposes through formal request, MTA agreement, and appropriate fee.
625
626 **Consent for publication**
627 Not applicable.
628
629 **Competing interests**
630 The authors declare that they have no competing interests.
631
632

633 References
634

635 1. Siegel, R.L., et al., *Cancer statistics, 2022.* CA Cancer J Clin, 2022. **72**(1): p. 7-33.

636 2. Guan, J., et al., *Therapeutic Ligands Antagonize Estrogen Receptor Function by*
637 *Impairing Its Mobility.* Cell, 2019. **178**(4): p. 949-963 e18.

638 3. Pan, H., et al., *20-Year Risks of Breast-Cancer Recurrence after Stopping Endocrine*
639 *Therapy at 5 Years.* N Engl J Med, 2017. **377**(19): p. 1836-1846.

640 4. McAndrew, N.P. and R.S. Finn, *Clinical Review on the Management of Hormone*
641 *Receptor-Positive Metastatic Breast Cancer.* JCO Oncol Pract, 2022. **18**(5): p. 319-327.

642 5. Varella, L. and M. Cristofanilli, *Evaluating Elacestrant in the Management of ER-*
643 *Positive, HER2-Negative Advanced Breast Cancer: Evidence to Date.* Onco Targets Ther,
644 2023. **16**: p. 189-196.

645 6. Menendez, J.A. and R. Lupu, *Fatty acid synthase and the lipogenic phenotype in cancer*
646 *pathogenesis.* Nat Rev Cancer, 2007. **7**(10): p. 763-77.

647 7. Menendez, J.A., et al., *Fatty Acid Synthase Confers Tamoxifen Resistance to*
648 *ER+/HER2+ Breast Cancer.* Cancers (Basel), 2021. **13**(5).

649 8. Schlaepfer, I.R., et al., *Progestin modulates the lipid profile and sensitivity of breast*
650 *cancer cells to docetaxel.* Mol Cell Endocrinol, 2012. **363**(1-2): p. 111-21.

651 9. Lopes-Coelho, F., S. Gouveia-Fernandes, and J. Serpa, *Metabolic cooperation between*
652 *cancer and non-cancerous stromal cells is pivotal in cancer progression.* Tumour Biol,
653 2018. **40**(2): p. 1010428318756203.

654 10. Blask, D.E., et al., *Circadian stage-dependent inhibition of human breast cancer*
655 *metabolism and growth by the nocturnal melatonin signal: consequences of its disruption*
656 *by light at night in rats and women.* Integr Cancer Ther, 2009. **8**(4): p. 347-53.

657 11. Jordan, V.C., *Tamoxifen as the first targeted long-term adjuvant therapy for breast*
658 *cancer.* Endocr Relat Cancer, 2014. **21**(3): p. R235-46.
659 12. Gruslova, A., et al., *FASN inhibition as a potential treatment for endocrine-resistant*
660 *breast cancer.* Breast Cancer Res Treat, 2021. **187**(2): p. 375-386.
661 13. Hultsch, S., et al., *Association of tamoxifen resistance and lipid reprogramming in breast*
662 *cancer.* BMC Cancer, 2018. **18**(1): p. 850.
663 14. Du, T., et al., *Key regulators of lipid metabolism drive endocrine resistance in invasive*
664 *lobular breast cancer.* Breast Cancer Res, 2018. **20**(1): p. 106.
665 15. Simigdala, N., et al., *Cholesterol biosynthesis pathway as a novel mechanism of*
666 *resistance to estrogen deprivation in estrogen receptor-positive breast cancer.* Breast
667 Cancer Res, 2016. **18**(1): p. 58.
668 16. Alò, P.L., et al., *Immunohistochemical expression of human erythrocyte glucose*
669 *transporter and fatty acid synthase in infiltrating breast carcinomas and adjacent*
670 *typical/atypical hyperplastic or normal breast tissue.* Am J Clin Pathol, 2001. **116**(1): p.
671 129-34.
672 17. Menendez, J.A. and R. Lupu, *Fatty acid synthase (FASN) as a therapeutic target in breast*
673 *cancer.* Expert Opin Ther Targets, 2017. **21**(11): p. 1001-1016.
674 18. Falchook, G., et al., *First-in-human study of the safety, pharmacokinetics, and*
675 *pharmacodynamics of first-in-class fatty acid synthase inhibitor TVB-2640 alone and*
676 *with a taxane in advanced tumors.* EClinicalMedicine, 2021. **34**: p. 100797.
677 19. Koundouros, N. and G. Poulogiannis, *Reprogramming of fatty acid metabolism in cancer.*
678 Br J Cancer, 2020. **122**(1): p. 4-22.

679 20. Finlay-Schultz, J., et al., *New generation breast cancer cell lines developed from patient-*
680 *derived xenografts.* Breast Cancer Res, 2020. **22**(1): p. 68.
681 21. Haughian, J.M., et al., *Maintenance of hormone responsiveness in luminal breast cancers*
682 *by suppression of Notch.* Proc Natl Acad Sci U S A, 2012. **109**(8): p. 2742-7.
683 22. Gendoo, D.M., et al., *Genefu: an R/Bioconductor package for computation of gene*
684 *expression-based signatures in breast cancer.* Bioinformatics, 2016. **32**(7): p. 1097-9.
685 23. Varshney, R., et al., *Neonatal intake of Omega-3 fatty acids enhances lipid oxidation in*
686 *adipocyte precursors.* iScience, 2023. **26**(1): p. 105750.
687 24. Rudolph, M.C., et al., *Mammalian fatty acid synthase activity from crude tissue lysates*
688 *tracing (1)(3)C-labeled substrates using gas chromatography-mass spectrometry.* Anal
689 Biochem, 2012. **428**(2): p. 158-66.
690 25. Rudolph, M.C., et al., *Thyroid hormone responsive protein Spot14 enhances catalysis of*
691 *fatty acid synthase in lactating mammary epithelium.* J Lipid Res, 2014. **55**(6): p. 1052-
692 1065.
693 26. Rudolph, M.C., et al., *Mammalian fatty acid synthase activity from crude tissue lysates*
694 *tracing 13C-labeled substrates using gas chromatography mass spectrometry.* Analytical
695 Biochemistry, 2012. **428**(2): p. 158-166.
696 27. Molenaar, M.R., et al., *LION/web: a web-based ontology enrichment tool for lipidomic*
697 *data analysis.* GigaScience, 2019. **8**(6).
698 28. Roshanzamir, F., et al., *Metastatic triple negative breast cancer adapts its metabolism to*
699 *destination tissues while retaining key metabolic signatures.* Proc Natl Acad Sci U S A,
700 2022. **119**(35): p. e2205456119.

701 29. Monaco, M.E., *Fatty acid metabolism in breast cancer subtypes.* Oncotarget, 2017. **8**(17):
702 p. 29487-29500.
703 30. Beloribi-Djefaflia, S., S. Vasseur, and F. Guillaumond, *Lipid metabolic reprogramming in*
704 *cancer cells.* Oncogenesis, 2016. **5**(1): p. e189.
705 31. Camarda, R., et al., *Inhibition of fatty acid oxidation as a therapy for MYC-*
706 *overexpressing triple-negative breast cancer.* Nat Med, 2016. **22**(4): p. 427-32.
707 32. Ahn, S., et al., *Metabolomic Rewiring Promotes Endocrine Therapy Resistance in Breast*
708 *Cancer.* Cancer Res, 2024. **84**(2): p. 291-304.
709 33. Vriens, K., et al., *Evidence for an alternative fatty acid desaturation pathway increasing*
710 *cancer plasticity.* Nature, 2019. **566**(7744): p. 403-406.
711 34. Alò, P.L., et al., *Fatty acid synthase (FAS) predictive strength in poorly differentiated*
712 *early breast carcinomas.* Tumori, 1999. **85**(1): p. 35-40.
713 35. Bobiński, R., et al., *Ferroptosis, Acyl Starvation, and Breast Cancer.* Mol Pharmacol,
714 2023. **103**(3): p. 132-144.
715 36. Lee, J.M., et al., *Fatty Acid Desaturases, Polyunsaturated Fatty Acid Regulation, and*
716 *Biotechnological Advances.* Nutrients, 2016. **8**(1).
717